Title

Vibrissal growth parameters of southern elephant seals Mirounga leonina: obtaining fine-scale, time-based stable isotope data

Authors

Lübcker, N
Condit, R
Beltran, RS
et al.

Publication Date

2016-11-09

DOI

10.3354/meps11899

Peer reviewed

Vol. 559: 243–255, 2016
doi: 10.3354/meps11899

MARINE ECOLOGY PROGRESS SERIES
Mar Ecol Prog Ser

Published November 9

Vibrissal growth parameters of southern elephant seals *Mirounga leonina*: obtaining fine-scale, time-based stable isotope data

Nico Lübcker[1,*], Richard Condit[2], Roxanne S. Beltran[3,4], P. J. Nico de Bruyn[1], Marthán N. Bester[1]

[1]Mammal Research Institute, Department of Zoology and Entomology, University of Pretoria, Private Bag X20, Hatfield 0028, Pretoria, South Africa

[2]Smithsonian Tropical Research Institute, Balboa, Panama City, 0843-03092, Panama

[3]Department of Biological Sciences, University of Alaska, Anchorage, AK 99508, USA

[4]Department of Biology and Wildlife, University of Alaska, Fairbanks, AK 99775, USA

ABSTRACT: Stable isotopes provide a powerful, indirect approach to assess the trophic ecology of individuals on a spatial and temporally integrated basis (especially when combined with telemetry). However, using stable isotopes requires accurate, species-specific quantification of the period of biomolecule deposition in the sampled tissue. Sequentially sampled vibrissae (whiskers) provide a chronology of biogeochemical data, although knowledge of vibrissal growth is required for temporal interpretations. We sampled vibrissae from southern elephant seals *Mirounga leonina* (hereafter SES) at Marion Island, southern Indian Ocean, to address the following aims: (1) define the prevalence and timing of their vibrissal replacement, (2) determine the vibrissal regrowth rate and temporal resolution of isotopic data captured along the length of sequentially sampled vibrissae, and (3) explore assumptions regarding their vibrissal growth. Contrary to the previously described asynchronous vibrissal shedding pattern of SES, 71.1% of individuals displayed vibrissal shedding during the annual pelage moult. Furthermore, vibrissal growth ceased once the asymptotic length was reached, and the vibrissae were retained before being replaced. Vibrissae with known growth histories were resampled at multiple known intervals to control for unknown growth starting dates. Vibrissae followed a von Bertalanffy growth function as the growth rate decreased near the asymptotic length. The resolution of the isotopic data obtainable per 2 mm section ranged from 3.5 d at the vibrissal tip to >40 d at the base. Using these defined growth rates and shedding patterns, researchers can prudently apply timestamps to stable isotope values along vibrissae.

KEY WORDS: Biomonitoring · Marine mammals · Moult · Pinnipeds · Shedding · Whiskers

INTRODUCTION

The combination of stable isotopes (SIs) and satellite-linked telemetry enables fine-scale, spatio-temporal dietary analyses, and biogeochemical habitat characterisations (Hobson et al. 2004, Jaeger et al. 2013, McMahon et al. 2013, Young et al. 2015, reviewed by Hussey et al. 2015). However, such a combined approach requires high-resolution SI data (Beltran et al. 2015, also see Banks et al. 2014). The SI signature captured along the length of keratinous tissue, such as feathers (Grecian et al. 2015), nails, hair or vibrissae, provides a time-series of the species' dietary history, if analysed chronologically (Hückstädt et al. 2012b, Robertson et al. 2013, Walters et al. 2014, Beltran et al. 2015). Numerous studies have

*Corresponding author: nlubcker@zoology.up.ac.za

focussed on ascertaining the exact species- and tissue-specific growth rates of slow-growing, biologically inert keratinous tissue of various species in different habitats (e.g. Greaves et al. 2004, Rohwer et al. 2009, Beltran et al. 2015).

The vibrissae (whiskers) of pinnipeds (Ling 1966) are particularly useful for dietary studies when using SI analysis (e.g. Hirons et al. 2001, Greaves et al. 2004, Zhao & Schell 2004, Hall-Aspland et al. 2005, Lewis et al. 2006, Cherel et al. 2009, Hindell et al. 2012, Walters et al. 2014, Rea et al. 2015). Vibrissae can be sampled relatively non-invasively and archive ecological information over longer temporal scales at a finer resolution than other tissues, such as blood (Tieszen et al. 1983). Whole blood, for example, has an isotopic turnover rate of ca. 1 mo (Tieszen et al. 1983), and consequently represents a single, integrated measurement of all the prey consumed during the month preceding sampling (e.g. Cherel et al. 2008, Boecklen et al. 2011). In contrast, the half-life of an isotopic tracer injected into captive harbour seals *Phoca vitulina* was 47.1 d (Zhao & Schell 2004), although isotopic changes were visible after 4 d, which implies that the marker incorporates rapidly into the protein synthesis of the growing vibrissae (Hirons et al. 2001). As a result, vibrissae are increasingly utilised to study the diet of pinnipeds (Greaves et al. 2004, Newland et al. 2011, Hindell et al. 2012, Hückstädt et al. 2012a,b, Walters et al. 2014). Nevertheless, the vibrissal growth rates of several phocid species remain to be determined, despite the recent interest in the utilisation of vibrissae to increase the temporal resolution of dietary data (e.g. Hirons et al. 2001, Greaves et al. 2004, Zhao & Schell 2004, Hall-Aspland et al. 2005, Beltran et al. 2015).

The growth rate and retention period of vibrissae vary between otariid and phocid species (Greaves et al. 2004). The vibrissae of otariids, such as Antarctic fur seals *Arctocephalus gazella* (Walters 2014) and Steller sea lions *Eumetopias jubatus* (Hirons et al. 2001), grow linearly and are retained for multiple years (Hirons et al. 2001, Cherel et al. 2009, Kernaléguen et al. 2012). In contrast, the vibrissae of phocids, such as grey seals *Halichoerus grypus* and *P. vitulina*, grow asymptotically and are characterised by an asynchronous growth and replacement pattern (Greaves et al. 2004, Hall-Aspland et al. 2005, Beltran et al. 2015). Furthermore, it has been suggested that vibrissae of phocids have short retention times; for example, *P. vitulina* and spotted seals *P. largha* shed their vibrissae on an annual basis (Zhao & Schell 2004, McHuron et al. 2016).

Southern elephant seals *Mirounga leonina* (hereafter SES) are the most abundant phocid in the sub-Antarctic region and, although their vibrissae have been used in dietary studies (Cherel et al. 2008, Newland et al. 2011, Hückstädt et al. 2012a, Walters et al. 2014), the growth rate and shedding pattern (Ling 1966) remains poorly understood. Whether the vibrissae of SES grow continuously before being replaced (Ling 1966), or enter an inactive phase after reaching the maximum length (Newland et al. 2011), remains debated. Also not yet enumerated, although generally accepted, is that individual vibrissae display asynchronous growth and replacement patterns (Ling 1966, Walters et al. 2014) (see Fig. S1 in the Supplement at www.int-res.com/articles/suppl/m559p243_supp.pdf). The ability to obtain fine-scale, temporally integrated biogeochemical data was demonstrated in a similar study conducted on a single captive adult female northern elephant seal *M. angustirostris* (Beltran et al. 2015). However, ascertaining the starting date of the vibrissal growth remains a prerequisite to assign dates to dietary data (Greaves et al. 2004). Resampling of vibrissal regrowths after initial sampling can help to account for unknown growth histories (e.g. Walters 2014).

The aim of this study was to: (1) determine the shedding phenology of SES vibrissae, (2) describe the vibrissal growth parameters and temporal range of data capture along the vibrissal regrowths of known-aged SES, (3) quantify the degree of inter-vibrissae isotopic variation to assess the degree of synchronous vibrissal growth, and (4) determine if the isotopic composition of the proximal sections of vibrissae are influenced by the presence of molecules other than pure keratin in the metabolically active inner vibrissal root sheath (Ling 1966, Hückstädt et al. 2012a). We hope to quantify the temporal resolution of isotopic data captured along the length of SES vibrissae and provide guidelines for future sampling. We additionally explore assumptions, that have been made in past studies, using samples collected from various age-class SES.

MATERIALS AND METHODS

Study site and data collection

Samples were collected at Marion Island in the southern Indian Ocean (46.88° S, 37.87° E) during the 2012/2013 and 2013/2014 breeding seasons and annual pelage moult, as part of the long-term (from 1983 ongoing) SES mark-recapture programme

(Bester & Wilkinson 1994, de Bruyn et al. 2008, Bester et al. 2011, Pistorius et al. 2011). All recently weaned SES born on Marion Island are marked in their hind flippers with uniquely numbered, colour-coded, plastic Dal 008 Jumbotags® (Dalton Supplies) for identification (de Bruyn et al. 2008, Pistorius et al. 2011). During the moult haulout (mid-August to mid-April), censused individuals were assigned to one of the following moult categories: unmoulted, <1/3 moulted, 1/3 to 2/3 moulted, >2/3 moulted, and fully moulted. For the purpose of this manuscript, 'moulting' describes the action of their annual pelage moult, while 'shedding' is used to describe the loss-replacement of SES vibrissae studied herein.

Timing and prevalence of vibrissal shedding

Body and snout photographs of marked individuals were routinely obtained as part of a concurrent photogrammetry study during the 2012/2013 and 2013/2014 moult periods (Postma et al. 2013). At each photograph sampling occasion, mystacial beds of each individual were assigned to one of the following vibrissal shedding categories: (1) not shed, when most of the anterior vibrissae were present and >4 of the posterior vibrissae were present on either side; (2) partially shed, when the anterior vibrissae were all shed but >4 of the posterior vibrissae were present on either side; or (3) completely shed, when ≤4 of the posterior vibrissae were present on either side of the face (Fig. 1, Figs. S1–S3 in the Supplement at www.int-res.com/articles/suppl/m559p243_supp.pdf). We also noted the number of cases where new vibrissal regrowths were visible (Fig. S4). We excluded males >3 yr old from analyses because adult males are rarely observed with a full set of vibrissae due to proboscis development and increased fighting (Ling 1966).

To avoid sampling biases due to the timing of the vibrissal shedding when calculating the prevalence of the observed shedding, animals were only included in the analysis if they were observed in at least 2 different moult stages during one moulting season. Furthermore, the individual should have been observed at least once at the onset of the annual pelage moult (i.e. unmoulted or <1/3 moulted) and once after (i.e. fully moulted). The vibrissal shedding status of an individual SES was then based on the progression from one state (not shed, partially shed or completely shed) to the next, in successive observations. For instance, if the individual was initially observed with a full vibrissal complement, then with a partially shed vibrissal aggregate, and recaptured on a third occasion with no vibrissae, we counted the individual's vibrissae as 'completely shed' during the moult. 'No shedding' occurred when the full vibrissal aggregate was observed during successive recaptures in one season. A non-parametric Kruskal-Wallis χ^2 test was utilised to identify any significant differences between the duration of the moult haulout and the number of observations between individuals that shed their vibrissae (completely or partially) and those that did not. The duration of the moult haulout for each individual was based on the number of days that elapsed between first and last recapture during the routinely conducted censuses, following Kirkman et al. (2003).

Growth rate of resampled vibrissae

To overcome the limitations of sampling vibrissae for which the onset of biomolecule deposition is unknown, we collected (by cutting as close to the skin as possible) the longest mystacial vibrissa from the right-hand side of recently weaned SES pups (ca. 22 to 24 d old). Vibrissa C1, C2 or D1 was sampled

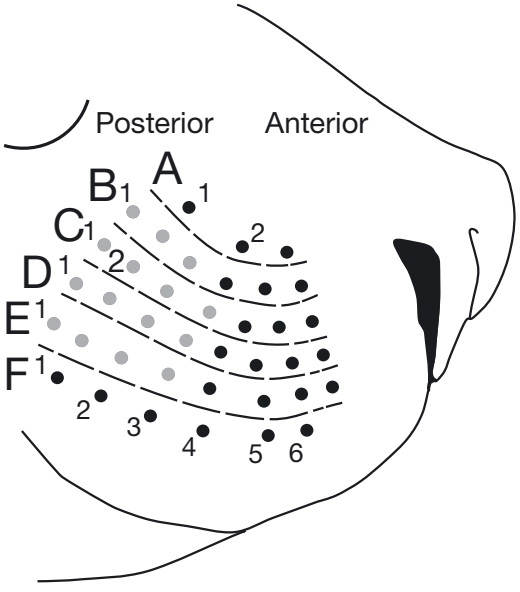

Fig. 1. Southern elephant seal *Mirounga leonina* (SES) mystacial vibrissal arrangement. The posterior vibrissae (grey circles) are more prominent than the anterior vibrissae (black circles), and can reach up to 160 mm in length. The diagram was modified from Sadou et al. (2014) following the description of the SES mystacial vibrissal arrangement in Ling (1966). Vibrissa C1, C2 or D1 was sampled from juvenile SES in order to determine their vibrissal regrowth rate. Vibrissae C1, C3, C4, and C5 were sampled on the left and right side of Seal 4 to assess the vibrissal growth synchronicity

(Fig. 1, Sadou et al. 2014). The collection date, vibrissa bed location and length of the initial 'cut-off' vibrissa were recorded for each tagged individual. A ruler was used to measure the length of the vibrissal regrowths of recaptured post-weaning SES (n = 101) on different occasions during the 60 d post-weaning period (Wilkinson & Bester 1990). After spending their first year foraging at sea (Kirkman et al. 2003), juveniles with visible regrowths were recaptured (n = 43) and the regrown vibrissae were again sampled by cutting as close to the skin as possible. These vibrissae were easily identified by their blunt distal ends (Fig. S5 in the Supplement).

Our starting assumption was that vibrissal regrowth in post-weaned SES was nonlinear, based especially on detailed vibrissal growth measurements of the closely related *Mirounga angustirostris* (Beltran et al. 2015). The vibrissal growth rate of *M. angustirostris* always decelerated until reaching the asymptotic length after about 1 yr (Beltran et al. 2015). The decay in growth rate was subsequently demonstrated using the widely applicable von Bertalanffy growth function (e.g. Hall-Aspland et al. 2005, Armstrong & Brooks 2013, Beltran et al. 2015). Although the growth rate model of Beltran et al. (2015) was based on an adult female, our preliminary results clearly demonstrated a similar decelerating growth pattern. We thus held the assumption that the von Bertalanffy growth model was our best option. Given decelerating growth, we needed at least 3 measurements to fit the model, and we included 19 juvenile SES for which we had ≥3 measurements that spanned a minimum of 200 d after weaning.

We fitted the von Bertalanffy function to the length of the vibrissae from all 19 animals jointly, treating the individual as a random effect. The model was thus specified by:

$$\text{Length} \sim \text{VonB}(\text{time} + \text{time}|\text{seal}) + \varepsilon \quad (1)$$

indicating that length was modelled as a function of time using the von Bertalanffy function, with the seal as a random effect, and a normally distributed error.

The general von Bertalanffy function is:

$$S_\rho(T) = A\left(1 - e^{-K(T-T_0)}\right) \quad (2)$$

where S_ρ represents the predicted length at time T given 3 parameters: A, asymptotic length; $K > 0$, the curvature parameter; and T_0, the time at which growth begins (so $S_\rho = 0$). Since we cut the vibrissae to the skin, we set $T_0 = 0$ and estimate only K and A. The model parameters include a fixed effect $\theta_F = (A_F, K_F)$, the best estimate for all 19 animals together (average), plus a separate set of parameters $\theta_i = (A_i, K_i)$, for each animal i. There must be a hyperdistribution for θ_i, describing the variance between animals, which we assumed to be bivariate Gaussian. To allow the Gaussian assumption, a log transformation for K was necessary because it is always a very small positive number, and a normal distribution would allow negative values. Thus, the fitted model parameters were log K and A, but we always back-transformed and display only K, not log K. The asymptote A was also constrained to be >0; however it never approached 0, so the Gaussian distribution is adequate. One additional parameter needed for the model was ε, or the residual standard deviation of the error around the model, again assumed to be Gaussian.

Estimating parameters required one likelihood function for the observations, describing the probability P_{ij} of observing the vibrissa of seal i on day j as size S_{ij}, given predicted size S_ρ based on the model and parameters θ_i for seal i, plus the residual Gaussian error:

$$P_{ij} = \text{dnorm}\left(S_{ij},\ \text{mean} = S_p(\theta_i),\ \text{SD} = \varepsilon\right) \quad (3)$$

where dnorm is the standard normal deviate given the mean and standard deviation (SD). Eq. (3) must be repeated for every measurement of every seal i, and the log-likelihood of all observations is $\sum_{ij} \log P_{ij}$.

There are 2 additional likelihood functions for the fixed effects, θ_F:

$$\begin{aligned} P_{Ai} &= \text{dnorm}(A_i, \text{mean} = A_f,\ \text{SD} = \sigma_A) \\ P_{\log K} &= \text{dnorm}\left(\log K, \text{mean} = \widehat{\log K},\ \text{SD} = \sigma_{\log K}\right) \end{aligned} \quad (4)$$

where A_f is the hyper-mean and σ_A are the hyper-SD of the asymptote lengths of 19 regrowths, and likewise for the hyper-mean and hyper-SD of $\log K$, $\widehat{\log K}$ and $\sigma_{\log K}$. The log of the 2 probabilities in Eq. (4) must be summed over each animal i. The total log-likelihood for the entire set of observations, given an entire set of parameters θ_i and θ_F, is:

$$\Pi = \sum_i \log P_{Ai} + \sum_i \log P_{\log K_i} + \sum_{ij} \log P_{ij} \quad (5)$$

Parameters were estimated in a Bayesian framework, using Metropolis updates based on the full likelihood formulation (Eq. 5). The entire set of parameters was updated 25 000 times, and the first 5000 were discarded as burn-in. The remaining 20 000 values describe posterior distributions for every parameter. Credible intervals (95%) for each were defined as the central 95 percentiles of these distributions. The individual parameters A_i and K_i were used to describe growth trajectories for the vibrissae of all 19 seals. In addition, given the von Bertalanffy formulation, with $T_0 = 0$, vibrissa growth rate at time T can be calculated as:

$$G_T = AKe^{(-KT)} \quad (6)$$

Posterior distributions of A_i and K_i were converted into posterior distribution of growth rates on Day 0 and Day 40 for each seal, with associated 95% credible intervals.

The resolution (number of days) represented by a 2 mm vibrissal segment was determined using:

$$T = \left[\frac{-1}{K}\ln\left(1 - \frac{S_T}{A}\right)\right] + T_0 \quad (7)$$

where S_T represents the length of the regrowth at time T (Beltran et al. 2015). Vibrissae are often subsampled into 2 mm segments for isotopic analyses (e.g. Newland et al. 2011, Walters et al. 2014), and we therefore reported the average number of days represented by a 2 mm vibrissal segment to emphasise the temporal resolution of the biogeochemistry data obtainable from sequentially sampled vibrissae.

We additionally used the length of the resampled regrowth to calculate the linear growth of the vibrissae for the 19 juvenile SES, for comparative purposes with Walters (2014).

Testing assumptions regarding vibrissal growth using stable isotopes

We assessed the $\delta^{13}C$ and $\delta^{15}N$ isotope profile captured along the length of previously unsampled vibrissa from a 1.7 yr old SES (hereafter, Seal 1) and a regrowth of a 1.1 yr old SES (hereafter, Seal 2) to confirm if: (1) the vibrissal growth is asynchronous; (2) vibrissae are retained for some period once their maximum length is reached; and (3) the maternally derived SI signatures are still observable in the vibrissae of juvenile SES.

To ensure that the SI signature is represented similarly across different vibrissae grown at the same time, we compared the SI profile of 2 vibrissae collected simultaneously from a third individual (hereafter, Seal 3, 0.8 yr old) and 8 vibrissae collected from a deceased adult female SES (hereafter Seal 4, Fig. 1) (see Lewis et al. 2006 and Newland et al. 2011). We controlled for different vibrissa lengths and growth rates in Seal 4 (Greaves et al. 2004, Beltran et al. 2015) by applying the growth rate of adult *M. angustirostris* from Beltran et al. (2015), using the maximum length of each of the sampled vibrissae as the asymptotic length in the equation.

Finally, to determine whether the vibrissae base is isotopically enriched due to the presence of molecules other than pure keratin, such as non-keratinised cortical cells (e.g. Hall-Aspland et al. 2005, Hückstädt et al. 2012a), we compared the isotopic signature of the base (10 mm) of the 8 vibrissae of Seal 4 to the adjacent 10 mm and to the most proximal 10 mm using a Kruskal-Wallis χ^2 test, followed by a post-hoc Wilcoxon rank sum test.

To prepare and analyse samples for stable isotopes, each vibrissa was cleaned using a chloroform:ethanol rinse as described by Lewis et al. (2006). All samples were then oven-dried for 24 h at 70°C (Lowther et al. 2013), sequentially sub-sampled into 2 mm sections ranging from the proximal portion (base) to the distal portion (tip) following Hindell et al. (2012) and Walters et al. (2014). The 2 mm section was again subsampled, and 0.5 to 0.6 mg segments were weighed into tin capsules (pre-cleaned in toluene) for SI analysis. The remaining portion was weighed as a duplicate, if a 0.5 to 0.6 mg sample was still available. Weighed sample aliquots were combusted in an elemental analyser (Flash EA, 1112 Series, Thermo™, Thermo Fisher Scientific), and the $\delta^{13}C$ and $\delta^{15}N$ isotopes were determined using a continuous-flow isotope ratio mass spectrometer (Delta V Plus, Thermo Finnigan) at the Stable Isotope Laboratory of the Mammal Research Institute, University of Pretoria, South Africa. Results are presented using standard delta notation in parts per thousand (‰) relative to an international standard: Vienna Pee Dee Belemnite (VPDB) for $\delta^{13}C$ and atmospheric N_2 (Air) for $\delta^{15}N$ (Coplen 1994).

Duplicate aliquots of samples were interspersed with an in-house standard (Merck gel) and blank after every 10 samples to ensure reproducibility. Reproducibility of $\delta^{13}C$ and $\delta^{15}N$ values based on the standards was <0.20‰, while the reproducibility of duplicate aliquots was ±0.20‰ for $\delta^{15}N$ and ±0.16‰ for $\delta^{13}C$ (n = 81 duplicates). The atomic C:N ratios are reported throughout the manuscript.

All statistical tests were performed in the R environment (R Core Team 2013). We tested normality using a Shapiro-Wilks normality test, while the *F*-test was used to compare the variances between variables, before applying an appropriate parametric (analysis of variance [ANOVA]) or non-parametric test (Kruskal-Wallis χ^2). Values are presented as mean ± 1 SD where applicable, and significance was assumed at $p < 0.05$.

RESULTS

Timing and prevalence of vibrissal shedding

From the total of 1289 facial photographs, 32.3 and 67.7% were conducted on males and females, re-

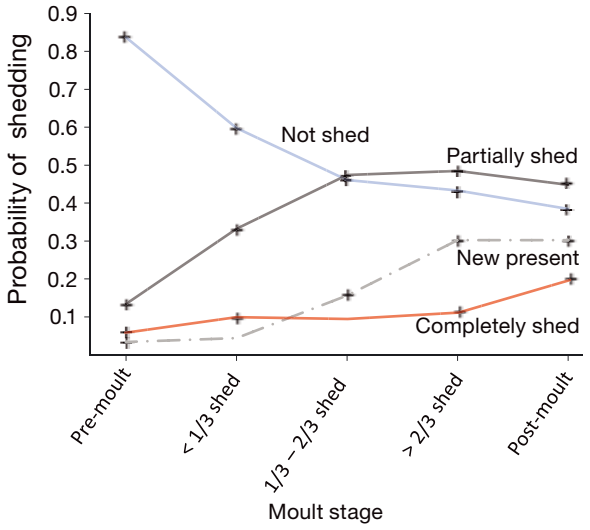

Fig. 2. Prevalence of southern elephant seal *Mirounga leonina* mystacial vibrissal shedding during each pelage moult stage. The probability of observing vibrissal shedding depended on pelage moult stage, and complete vibrissal shedding (red line) occurred most frequently at the end of the pelage moult

spectively. Poor photo resolution, unknown moult stage, or obstruction of the vibrissae resulted in the exclusion of 162 observations. During the 30.1 ± 9.7 d moulting period, 62.3% of the complete vibrissal shedding observations occurred during the post-moult stage (Fig. 2). The probability of observing vibrissal shedding was strongly related to the pelage shedding stage (Fig. 2), suggesting that the timing of vibrissal shedding should be accounted for when calculating its prevalence.

The prevalence of vibrissal shedding was based on 201 individuals (549 observations), consisting of 1 to 3 yr old juvenile males (23.9% of individuals), juvenile females (23.4%) and adult females >3 yr old (52.7%). Of the 201 individuals, 71.1% displayed signs of vibrissal shedding during the annual moult (Fig. S6 in the Supplement at www.int-res.com/articles/suppl/m559p243_supp.pdf). The vibrissae were completely shed in 22.5% of the individuals and partially shed in 48.5%. Only 28.9% of the individuals retained their vibrissae during the annual pelage moult. New vibrissal growths were observed in 56.4% of individuals that shed their vibrissae. The prevalence of vibrissal shedding was highest in age 2 individuals, with 59.2% completely shedding their vibrissae (Fig. S6). The sighting probability and moult duration did not differ significantly (Kruskal-Wallis $\chi^2 = 1.38$, df = 4, p = 0.85; Kruskal-Wallis $\chi^2 = 32.93$, df = 39, p = 0.74, respectively) between individuals that completely, or partially, shed their vibrissae and individuals that did not. Individuals that shed their vibrissae were observed 2.9 ± 0.8 times within a given moult season; similar to the 2.6 ± 0.7 times of those that did not shed their vibrissae. The duration of the moult of individuals that shed their vibrissae (30.3 ± 9.9 d) was also similar to that of individuals that did not (29.0 ± 7.9 d). One individual (hereafter, Seal 5) that completely shed all its vibrissae during the moult was recaptured 138 d later with a full vibrissal complement (Fig. S7 in the Supplement).

Growth rate of resampled vibrissae

The vibrissal regrowth rate of the known-aged SES (n = 19) represents a von Bertalanffy growth function (Fig. 3): the vibrissal regrowth rate decreases exponentially $[G_t = 77.1\,(0.00744)(e^{-0.00744t})]$, following from Eq. (6). Results were reported as the mean, followed by the 95% credible intervals (lower 95 percentile; upper 95 percentile in brackets), where applicable. The resampled regrowths were shorter (66.3 ± 12.2 mm) than the vibrissae originally cut off (75.7 ± 9.7 mm), while also shorter than the predicted A of the regrowths (77.1 [65.4; 89.9] mm), therefore suggesting that the vibrissal regrowths were still actively growing when sampled. The predicted K of the resampled regrowths was 0.00744 (0.0058; 0.0095).

The maximum growth rate (0.57 [0.47; 0.67] mm d^{-1}) occurred directly after sampling the initial vibrissae ($T_0 = 0$), and decreased to 0.42 (0.37; 0.48) mm d^{-1} after growing ca. 20 mm in 40 d (Table 1). The mean number of days represented by a 2 mm vibrissal segment when sampled was therefore 3.5 d (ranging from 2.4 to 5.5 d based on 95% percent credibility intervals), and increased to 4.0 d (ranging from 3.5 to 6.3 d) after 40 d. The daily resolution decreased further towards the base of the vibrissae, averaging 10.3 d (ranging from 5.4 to 24.0 d) after growing ca. 52 mm, 150 d after the initial sampling. When regrowth approached A, the resolution of the dietary data obtainable near the base of the regrowth was reduced to the average isotopic signature of all the prey consumed over the >40 d period. Irrespectively, the estimated growth rate from a simple linear regression was 0.19 ± 0.06 mm d^{-1}.

Testing assumptions regarding vibrissal growth using stable isotopes

Two vibrissae, each sub-sampled into 51 (Seal 1) and 35 segments (Seal 2), were used to assess the

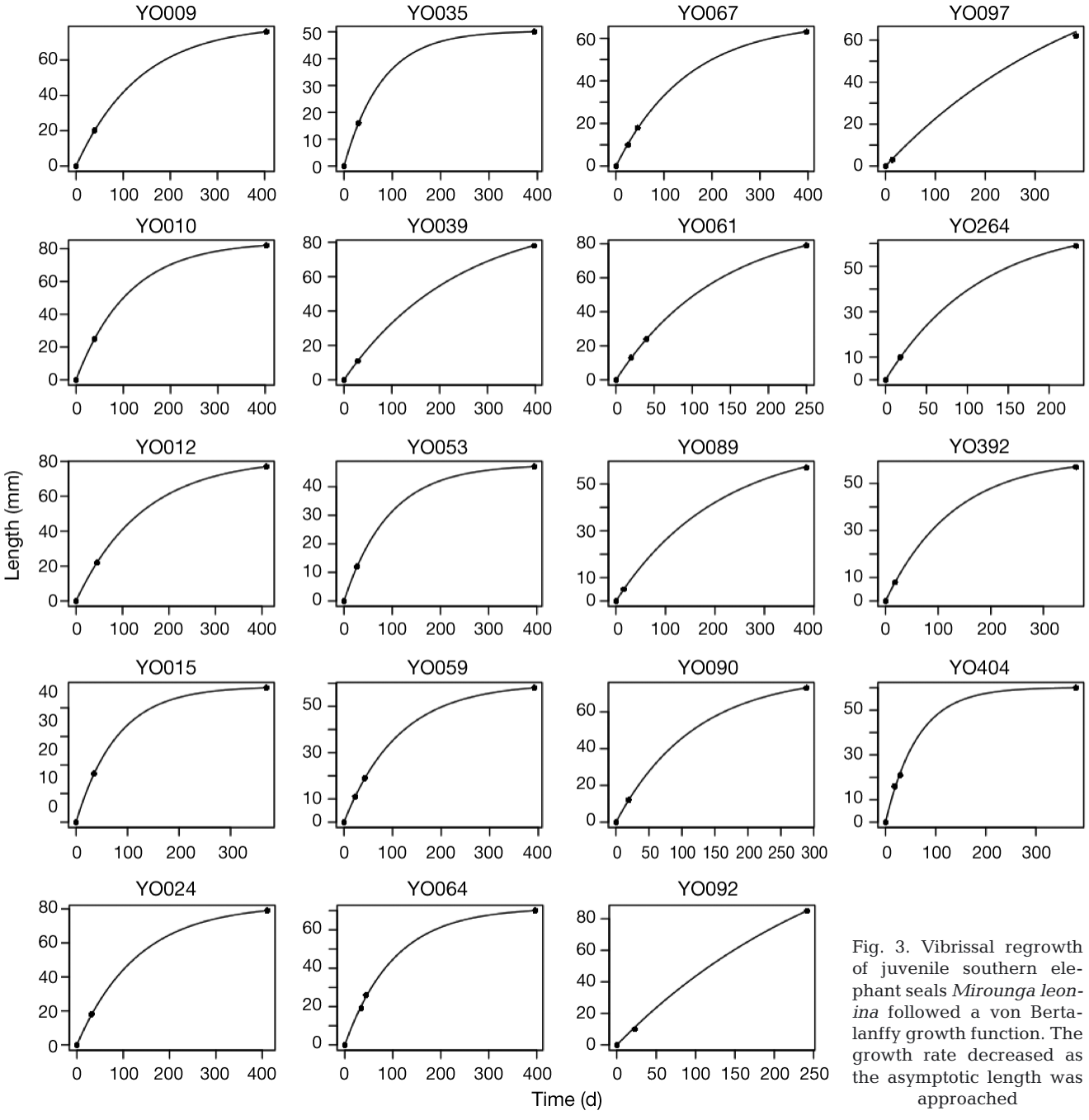

Fig. 3. Vibrissal regrowth of juvenile southern elephant seals *Mirounga leonina* followed a von Bertalanffy growth function. The growth rate decreased as the asymptotic length was approached

retention of the vibrissae in juvenile SES. The maternal signature was still present in the full vibrissa of Seal 1 at 1.7 yr old (n = 51 samples), as well as in the regrowth sampled from the 1.1 yr old Seal 2 (n = 35 samples) before the second moult (Fig. 4), confirming that the vibrissae grew asynchronously and that they were retained for some period once their maximum length was reached. The maternal signature, and subsequent $\delta^{15}N$ depletion, represented 83% of the total length of the vibrissa collected from Seal 2. Independent foraging was represented by 17% of the vibrissal regrowth of Seal 2, while only by the last segment of Seal 1 (Fig. 4).

The $\delta^{15}N$ (10.6 ± 1.2‰) and $\delta^{13}C$ (–20.1 ± 0.2‰) profiles along the regrowth of Seal 3 were nearly identical to the $\delta^{15}N$ (10.7 ± 1.4‰) and $\delta^{13}C$ (–19.9 ± 0.3‰) profiles of the duplicate regrowth (Fig. 5).

Finally, the vibrissae collected from Seal 4 were used to assess the degree of synchronous vibrissal growth expected if the vibrissae were replaced syn-

Table 1. Estimates of the asymptotic length (A) and the growth curvature constant (K) of individual southern elephant seal *Mirounga leonina* (SES) vibrissal regrowths (n = 19). The growth rate at time T = 0 d and after 40 d are also presented. The reported values represent the mean and 95% credibility intervals (in brackets) of the parameters. The estimated growth parameters for one individual (YO092) were out of range of the maximum vibrissal length measured in SES

Seal ID	K (d^{-1})	A (mm)	Growth rate	
			T = 0 d	T = 40 d
YO009	0.00736 (0.0068, 0.0080)	80.1 (78.4, 81.9)	0.590 (0.55, 0.63)	0.440 (0.42, 0.46)
YO010	0.00899 (0.0084, 0.0096)	84.3 (82.8, 85.7)	0.758 (0.72, 0.80)	0.529 (0.51, 0.55)
YO012	0.00696 (0.0064, 0.0075)	81.7 (79.8, 83.7)	0.568 (0.53, 0.61)	0.430 (0.41, 0.45)
YO015	0.01260 (0.0114, 0.0138)	47.5 (46.2, 48.8)	0.599 (0.55, 0.65)	0.361 (0.34, 0.38)
YO024	0.00767 (0.0070, 0.0084)	82.6 (80.8, 84.4)	0.633 (0.58, 0.69)	0.466 (0.44, 0.49)
YO035	0.01269 (0.0115, 0.0140)	50.4 (49.1, 51.6)	0.643 (0.59, 0.70)	0.385 (0.37, 0.40)
YO039	0.00420 (0.0034, 0.0049)	96.3 (90.1, 104.9)	0.404 (0.36, 0.45)	0.341 (0.31, 0.37)
YO053	0.01070 (0.0094, 0.0120)	47.7 (46.5, 49.1)	0.513 (0.46, 0.57)	0.332 (0.31, 0.35)
YO059	0.00885 (0.0082, 0.0095)	59.9 (58.5, 61.4)	0.531 (0.50, 0.57)	0.372 (0.36, 0.39)
YO064	0.00975 (0.0092, 0.0103)	71.5 (70.2, 72.9)	0.698 (0.66, 0.73)	0.472 (0.46, 0.48)
YO067	0.00668 (0.0061, 0.0073)	67.9 (66.0, 69.9)	0.453 (0.43, 0.48)	0.347 (0.33, 0.36)
YO081	0.00739 (0.0067, 0.0080)	93.8 (90.6, 98.1)	0.694 (0.65, 0.73)	0.515 (0.50, 0.53)
YO089	0.00482 (0.0035, 0.0066)	68.1 (61.6, 77.5)	0.330 (0.27, 0.40)	0.271 (0.23, 0.31)
YO090	0.00845 (0.0071, 0.0098)	80.1 (77.1, 84.0)	0.678 (0.60, 0.76)	0.482 (0.45, 0.51)
YO092	0.00332 (0.0027, 0.0043)	154.3 (131.3, 177.7)	0.511 (0.48, 0.56)	0.446 (0.43, 0.47)
YO097	0.00236 (0.0015, 0.0047)	107.7 (74.1, 145.6)	0.252 (0.21, 0.35)	0.226 (0.20, 0.29)
YO264	0.00860 (0.0068, 0.0102)	68.4 (64.6, 74.3)	0.593 (0.51, 0.66)	0.416 (0.39, 0.44)
YO392	0.00774 (0.0064, 0.0093)	60.9 (58.5, 63.9)	0.472 (0.40, 0.54)	0.345 (0.32, 0.38)
YO404	0.01557 (0.0146, 0.0166)	60.2 (59.0, 61.4)	0.938 (0.88, 0.99)	0.502 (0.49, 0.51)

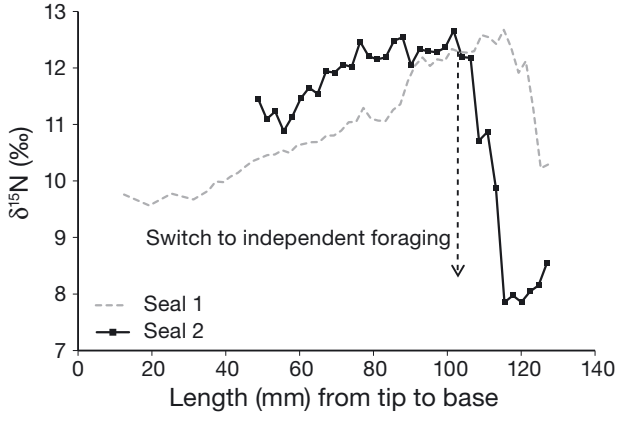

Fig. 4. Pre-foraging trip isotopic signature and subsequent ca. 3.0‰ $\delta^{15}N$ decrease from nursing to independent foraging (Walters et al. 2014) was still observable in 1.7 and 1.1 yr old southern elephant seals *Mirounga leonina* (Seals 1 and 2, respectively). No evidence of a secondary growth spurt or continuous growth to offset abrasion was observed

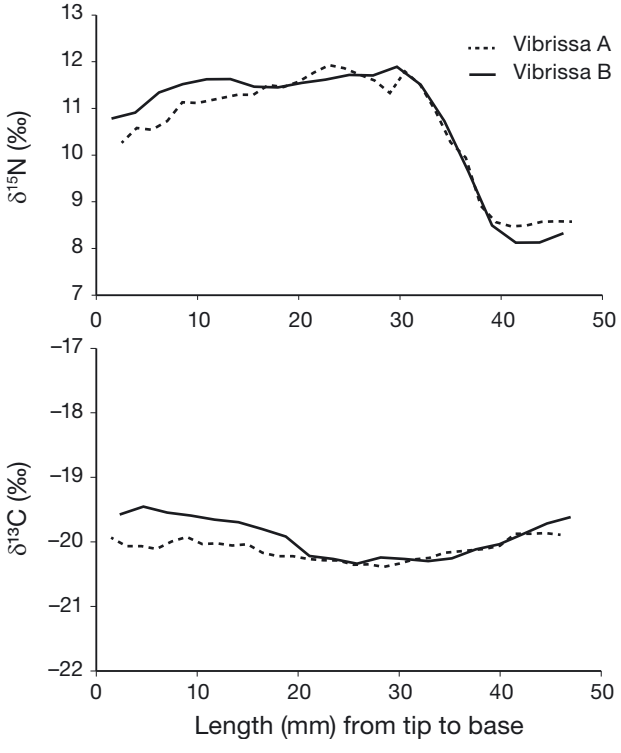

Fig. 5. Synchronously grown vibrissal regrowths sampled from the same individual southern elephant seal *Mirounga leonina* (Seal 3) were nearly identical, confirming that the stable isotopes are similarly incorporated in different vibrissae

chronously. The 8 vibrissae plucked from Seal 4 ranged from 73 to 165 mm in length and were sectioned into 352 total segments for SI analysis. The $\delta^{15}N$ ranged from 8.4 to 11.6‰ (9.7 ± 0.6‰) and the $\delta^{13}C$ from −19.4 to −21.7‰ (−20.3 ± 0.5‰). Significant differences in both $\delta^{15}N$ and $\delta^{13}C$ were detected among vibrissae ($\delta^{15}N$: Kruskal-Wallis χ^2 = 64.4, df =

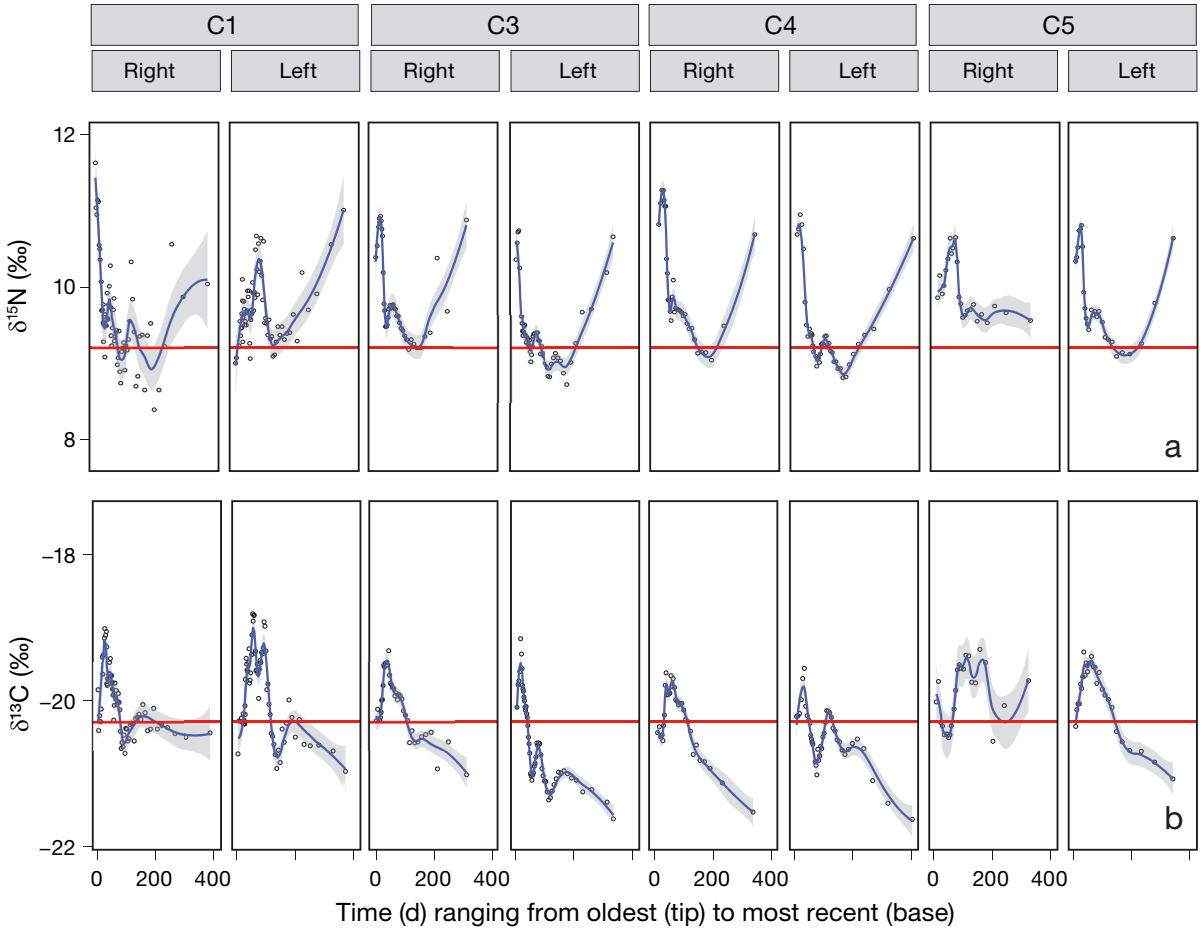

Fig. 6. Time-series of $\delta^{15}N$ and $\delta^{13}C$ capture along the length of 8 different vibrissae sampled from a dead adult female southern elephant seal *Mirounga leonina* (Seal 4). A Lowess smoothing algorithm was applied (grey). The arbitrary red line was added to ease comparison. The stable isotope patterns of complementary vibrissae were similar

7, $p < 0.001$; $\delta^{13}C$: Kruskal-Wallis $\chi^2 = 74.4$, df = 7, $p < 0.001$). However, similarities in both $\delta^{15}N$ and $\delta^{13}C$ between different vibrissae were obvious for Right C3, Right C4 and Left C5 (Fig. 6), and the $\delta^{15}N$ pattern did not vary between most of the vibrissae, except for Right C1 and Right C5. The inter-vibrissal variation observable in $\delta^{13}C$ was also low: Right C5 had a unique $\delta^{13}C$ profile compared to the rest of the vibrissae.

Significant isotopic differences were detected between the proximal 10 mm, the adjacent 10 mm, and the most distal 10 mm of the vibrissae ($\delta^{15}N$: Kruskal-Wallis $\chi^2 = 52.3$, df = 2, $p < 0.001$; $\delta^{13}C$: Kruskal-Wallis $\chi^2 = 36.0$, df = 2, $p < 0.001$; C:N: Kruskal-Wallis $\chi^2 = 14.5$, df = 2, $p < 0.001$) (Fig. S8 in the Supplement). The C:N at the base and tip of vibrissae did not differ significantly ($p = 0.86$).

The atomic C:N ratio of all the vibrissal segments analysed (n = 596) was 3.7 ± 0.1.

DISCUSSION

Timing and prevalence of vibrissal shedding

Southern elephant seals show a greater probability of shedding most of their vibrissae during the annual moult than of retaining them. This finding contradicts the long-standing notion that SES vibrissae are shed asynchronously (Ling 1966). The timing of the SES synchronous vibrissal shedding was strongly related to the moult stage, being the highest near the completion of the moult (Fig. 2). Yet, inter-individual variation in the vibrissal shedding during the moult precludes the inference of general assumptions regarding the growth history of fully grown vibrissae. This variability is likely due to the trade-offs between functionality and the need for replacement. Mammalian vibrissae function as individual, highly sensitive sensory organs vital to foraging success, and an

asynchronous loss-replacement strategy presumably allows for sustained functionality (Ling 1966, Greaves et al. 2004, Newland et al. 2011, Beltran et al. 2015). On the other hand, the moult may provide a period when vibrissae are redundant, given the land-based fasting typical of this species.

In this study, no individuals completely shed their vibrissae during the first moult (age 1) (Fig. S6 in the Supplement). In contrast, the majority of 2 yr old SES completely shed their vibrissae, consistent with the notion that phocid vibrissae can be retained for 2 yr before being replaced (Ling 1966, Beltran et al. 2015). Previous studies have suggested that full replacement of phocid vibrissae takes about 1 yr (Hirons et al. 2001, Lewis et al. 2006, Beltran et al. 2015), although naturally shed vibrissae can regrow in less than a full year (Newland et al. 2011, Hückstädt et al. 2012a, Walters et al. 2014). New vibrissal regrowths were visible in 56.4 % of all the individuals that shed vibrissae during the 30.1 ± 9.7 d moulting period, suggesting that vibrissae can grow back rapidly (Fig. S4). One individual (Seal 5) that completely shed all of its vibrissae was recaptured 138 d later with a full, although potentially still growing, vibrissal complement (Fig. S7). Opportunistically sampled, fully grown vibrissae can, therefore, be up to 2 yr old, but could have grown at any time.

Vibrissae that are shed and replaced simultaneously should incorporate a similar SI pattern along their lengths (e.g. Lewis et al. 2006). However, Hückstädt et al. (2012a) and Newland et al. (2011) found contrasting results and subsequently described the results of Lewis et al. (2006) as a sampling artefact. Nevertheless, the variable shedding patterns and similarities in isotopic signatures observed in some, but not all, vibrissae from Seal 4, help to explain the discrepancy between previous findings (Fig. 6). Some of the vibrissae of Seal 4 appear to have grown synchronously after being shed. Nonetheless, we still have to assume the onset of the growth history of any randomly sampled vibrissa from an individual (especially considering the variability in the shedding probability between different aged SES, Fig. S6).

Growth rate of resampled vibrissae

To control for unknown start and end dates of the biomolecule deposition (i.e. sampling vibrissae with unknown growth histories), we applied the von Bertalanffy growth function (von Bertalanffy 1938) to resampled vibrissae. With a Bayesian modelling approach, the vibrissal regrowth rate of the juvenile SES was shown to follow a nonlinear growth function with the growth rate decreasing as a function of length (Fig. 3). The temporal resolution obtainable from the 2 mm vibrissal segments decreased exponentially from the tip (3.5 d) to the base of the vibrissae (>40 d) as the growth rate decreased. The vibrissal regrowths were predicted to enter an inactive phase once the asymptotic length is reached, and had a similar lifespan to the vibrissae of *Mirounga angustirostris* (ca. 369 d) (Beltran et al. 2015). Nevertheless, the vibrissal regrowths were still actively growing when sampled, spanning the entire 363 ± 60.2 d of their first year spent at sea.

The vibrissal growth rate of pinnipeds ranges from 0.08 to 0.87 mm d^{-1} (Hirons et al. 2001, Greaves et al. 2004, Zhao & Schell 2004, Hall-Aspland et al. 2005, Hindell et al. 2012).The SES vibrissal regrowth rates were within the predicted range of previous studies (Table 1). However, the regrowth rate of the juvenile SES vibrissae (K = 0.00744 d^{-1}, A = 77.1 mm) was higher than measured in other phocids, such as captive juvenile grey seals *Halichoerus grypus* (K = 0.0024 d^{-1}, range = 0.0019–0.0030, A = 58.0 mm) (Greaves et al. 2004), a captive adult *M. angustirostris* (K = 0.00132 d^{-1}, range = 0.0045–0.00323, A = 81.7 mm) (Beltran et al. 2015) and adult leopard seals *Hydrurga leptonyx* (K = 0. 0032 d^{-1}, A = 72.0 mm) (Hall-Aspland et al. 2005). Still, the growth rate estimated from the simple linear regression was identical to that from the only other study of the vibrissal growth rate of juvenile SES (0.19 mm d^{-1}, range 0.10–0.25) (Walters 2014), and similar to that of harbour seals *Phoca vitulina* (up to 0.78 mm d^{-1}) (Zhao & Schell 2004). However, the growth rate predicted by the von Bertalanffy growth function was higher than estimated by the simple linear model due to the nonlinearity in growth (present study). Given the nonlinear vibrissal growth rate, studies that relied on the presence of cyclic markers (e.g. annual fasting events or glycine markers) to measure the vibrissal growth rate of phocids might be unreliable, as they assumed that vibrissal growth is linear and continuous (e.g. Hirons et al. 2001, Zhao & Schell 2004, Walters 2014); similarly noted by Greaves et al. (2004) and Hall-Aspland et al. (2005).

In the present study, inter-individual variation in the vibrissal regrowth rate was also evident (Fig. 3). This may be constrained by the timing of the regrowth length measurements and sampling of vibrissae with different asymptotic lengths. Three or more measurements per individual are required to fit a non-linear vibrissal growth rate model. Furthermore,

vibrissae situated at different positions in the vibrissae bed-map have different A and K values, which should be accounted for (e.g. Beltran et al. 2015). We sampled 1 of 3 mystacial vibrissae (Fig. 1) due to the logistical challenge of sampling the same vibrissa from exactly the same position from different individuals in a wild population. This potentially contributed to the observed inter-individual variation in the vibrissal growth rates. Nevertheless, the resolution of dietary information obtainable with regrowths is higher than that obtainable from, e.g. blood, hair or any other tissue type collected from SES while foraging at sea for extended periods of time.

Sampling considerations

Several unknowns regarding vibrissal growth remain. For instance, the increased somatic body growth of the pups could accelerate vibrissal regrowth rate, as observed in vibrissal regrowths collected from recently weaned bearded seal *Erignathus barbatus* pups (0.87 ± 0.24 mm d^{-1}) (Hindell et al. 2012). Yet, the presence of the characteristic 3.4‰ $\delta^{15}N$ depletion from dependent nursing to independent foraging that was observable in the vibrissae of a 1.7 yr old SES sampled at Marion Island confirmed that: (1) the vibrissa growth ceases once the asymptotic length is reached, whereafter the growth enters a telogen phase; and (2) their vibrissae are retained once the maximum length is reached before being replaced (Fig. 3). This finding, and the unpredictable vibrissal growth histories of SES, suggests that the assumptions of previous studies might be invalid (e.g. Newland et al. 2011, Hückstädt et al. 2012a). Newland et al. (2011), for example, utilised randomly selected 2 mm vibrissa segments of 1 to 3 yr old SES to study the diet of juvenile SES at Macquarie Island (1999 to 2000). Yet, herein we demonstrate that the enriched $\delta^{15}N$ maternal signature, and subsequent $\delta^{15}N$ depletion at the onset of independent foraging (Walters et al. 2014), represents the majority of the vibrissae sampled from SES up to 1.7 yr old (and perhaps older), questioning their findings. The resampling of vibrissal regrowths not only accounts for growth history of the vibrissae, but also increases the portion of the vibrissa that represents independent foraging (Fig. 4). Walters et al. (2014) sampled vibrissae of ca. 0.8 yr old SES at Macquarie Island (54.6167° S, 158.8500° E), and merely 9.1% of the total length of the vibrissae sampled from n = 7 out of 12 SES represented independent foraging. The portion representing independent foraging in the other individuals was still beneath the skin (Walters et al. 2014), similarly observed in the vibrissa of the previously unsampled Seal 1 (Fig. 4).

In the present study, the longer, posterior vibrissae were generally retained, suggesting that the shorter vibrissae are more readily replaced (also see Ling 1966, Walters et al. 2014). Sampling the shorter, anterior (front) vibrissae, as suggested by Walters et al. (2014) and Beltran et al. (2015), increases the likelihood of it still being actively growing. Nonetheless, no accurate temporal interpretation of randomly sampled vibrissae is plausible if the growth histories are unknown. The sampling of vibrissae from juvenile SES should preferably occur as close as possible to departure on their post-weaning foraging trip, and regrowths can be resampled at the onset of their first obligatory moult.

The ca. 12 mm portion left embedded when sampling the initial vibrissa captured the slowest part of the growth. This 12 mm portion could potentially represent ca. 130 d growth (estimated from the von Bertalanffy growth function), which should be accounted for. The maximum vibrissal growth rate occurred directly after cutting, but is represented 12 mm from the tip of the new regrowth due to the embedded 12 mm portion which had grown according to the initial vibrissa's growth curve (see Hall-Aspland et al. 2005).

Plucking vibrissal regrowths instead of cutting would add additional dietary information captured in the embedded 12 mm portion. Nevertheless, the cortical cells at the base of the vibrissae keratinise just above the bulb region of the follicle (within the internal root sheath) (Ling 1966), suggesting that the basal segment is still biologically active (growing) and does not represent pure keratin. As a result, the basal segments are mostly excluded from analyses (Hall-Aspland et al. 2005, Hückstädt et al. 2012a, Beltran et al. 2015), suggesting that vibrissae plucking during sampling might be unnecessary. Although we found significant differences in the SI ratios between the base and the adjacent 10 mm of the vibrissae, similar differences between the base and the tip (Fig. S8 in the Supplement) suggest that the variation might be caused by other biologically relevant factors, such as transition from active foraging to fasting during long distance migrations (e.g. Hückstädt et al. 2012a), and requires further enquiry.

Lastly, when comparing the SI signature captured along the length of different vibrissae, it is assumed that the SI signature is incorporated similarly. The high reproducibility of the SI signature captured along the length of 2 synchronously grown vibrissal regrowths (Fig. 5), and the vibrissae of Seal 4 (Fig. 6),

suggest that SI deposition is similar in different vibrissae with different growth rates (i.e. equal isotopic routing).

Conclusion

The use of vibrissal regrowths represents a feasible matrix for obtaining temporally integrated biogeochemical information. In general, the retention and shedding cycle of the vibrissae appears to be species- and individual-specific (Ling 1966, Greaves et al. 2004, Beltran et al. 2015). Although synchronous vibrissal shedding can occur in some individuals as demonstrated, no generalisation should be made regarding the period of biomolecule deposition in any vibrissae with an unknown growth history. In combination with the unpredictable, asynchronous loss-replacement pattern (Ling 1966, Beltran et al. 2015), this hinders any verification of commencement of growth. Therefore, the growth history of vibrissae should be reset before temporal dietary interpretations are attempted. This study advances our capacity to interpret the interaction between predators and their environment on a biologically significant temporal scale.

Acknowledgements. Field personnel followed the guidelines for handling and treatment of marine mammals in field research supported by the Society for Marine Mammalogy (Gales et al. 2009). The tagging and handling of seals at Marion Island are carried out under the provisions of the South African Sea Birds and Seals Protection Act, 1973 (Act 46, 1973), the Marine Living Resources Act, 1998 (Act 18 of 1998) and the Prince Edward Islands Management Plan. The project has ethics clearance from the Animal Use and Care Committee (AUCC) of the Faculty of Veterinary Science, University of Pretoria, under AUCC 040827-022, AUCC 040827-023, AUCC 040827-024 and EC030602-016 and is carried out under permit from the Director-General: Department of Environmental Affairs, South Africa. Funding was provided by the South African Department of Science and Technology, through the National Research Foundation (NRF), within the South African National Antarctic Programme (SANAP). The Department of Environmental Affairs (DEA) provided logistical support at Marion Island. The opinions and conclusions drawn and discussed are attributed to the authors and not necessarily to the NRF. We thank the various dedicated collaborators, as well as field and laboratory assistants, in particular, Wiam Haddad, Mia Wege, Hennie Louw, Christiaan Brink, Frikkie van der Vyver, Dr Grant Hall, Nicolas Prinsloo, André van Tonder, Tanita Cronje, Inger Fabris-Rotelli and Christine Kraamwinkel.

LITERATURE CITED

Armstrong DP, Brooks RJ (2013) Application of hierarchical biphasic growth models to long-term data for snapping turtles. Ecol Modell 250:119–125

Banks J, Lea MA, Wall S, McMahon CR, Hindell MA (2014) Combining bio-logging and fatty acid signature analysis indicates spatio-temporal variation in the diet of the southern elephant seal, *Mirounga leonina*. J Exp Mar Biol Ecol 450:79–90

Beltran RS, Sadou MC, Condit R, Peterson SH, Reichmuth C, Costa DP (2015) Fine-scale whisker growth measurements can reveal temporal foraging patterns from stable isotope signatures. Mar Ecol Prog Ser 523: 243–253

Bester MN, Wilkinson IS (1994) Population ecology of southern elephant seals *Mirounga leonina* at Marion Island. In: Le Boeuf BJ, Laws RM (eds), Elephant seals, population ecology, behavior, and physiology. University of California Press, Berkeley, p 85–97

Bester MN, de Bruyn PJN, Oosthuizen WC, Tosh CA, McIntyre T, Reisinger RR, Wege M (2011) The Marine Mammal Programme at the Prince Edward Islands: 38 years of research. Afr J Mar Sci 33:511–521

Boecklen WJ, Yarnes CT, Cook BA, James AC (2011) On the use of stable isotopes in trophic ecology. Annu Rev Ecol Evol Syst 42:411–440

Cherel Y, Ducatez S, Fontaine C, Richard P, Guinet C (2008) Stable isotopes reveal the trophic position and mesopelagic fish diet of female southern elephant seals breeding on the Kerguelen Islands. Mar Ecol Prog Ser 370: 239–247

Cherel Y, Kernaléguen L, Richard P, Guinet C (2009) Whisker isotopic signature depicts migration patterns and multi-year intra- and inter-individual foraging strategies in fur seals. Biol Lett 5:830–832

Coplen TB (1994) Reporting of stable hydrogen, carbon, and oxygen isotopic abundances. Pure Appl Chem 66: 273–276

de Bruyn PJN, Tosh CA, Oosthuizen WC, Phalanndwa MV, Bester MN (2008) Temporary marking of unweaned southern elephant seal (*Mirounga leonina* L.) pups. S Afr J Wildl Res 38:133–137

Gales NJ, Bowen WD, Johnston DW, Kovacs KM and others (2009) Guidelines for the treatment of marine mammals in field research. Mar Mamm Sci 25:725–736

Greaves DK, Hammill MO, Eddington JD, Pettipas D, Schreer JF (2004) Growth rate and shedding of vibrissae in the gray seal, *Halichoerus grypus*: A cautionary note for stable isotope diet analysis. Mar Mamm Sci 20: 296–304

Grecian WJ, McGill RAR, Phillips RA, Ryan PG, Furness RW (2015) Quantifying variation in $\delta^{13}C$ and $\delta^{15}N$ isotopes within and between feathers and individuals: Is one sample enough? Mar Biol 162:733–741

Hall-Aspland SA, Rogers TL, Canfield RB (2005) Stable carbon and nitrogen isotope analysis reveals seasonal variation in the diet of leopard seals. Mar Ecol Prog Ser 305: 249–259

Hindell MA, Lyderson C, Hop H, Kovacs KM (2012) Pre-partum diet of adult female bearded seals in years of contrasting ice conditions. PLOS ONE 7:e38307

Hirons AC, Schell DM, Aubin DJ (2001) Growth rates of vibrissae of harbor seals (*Phoca vitulina*) and Steller sea lions (*Eumetopias jubatus*). Can J Zool 79:1053–1061

Hobson KA, Sinclair EH, York AE, Thomason JR, Merrick RE (2004) Retrospective isotopic analyses of Steller sea lion tooth annuli and seabird feathers: A cross-taxa approach to investigating regime and dietary shifts in the Gulf of Alaska. Mar Mamm Sci 20:621–638

Hückstädt LA, Koch PL, McDonald BI, Goebel ME, Crocker DE, Costa DP (2012a) Stable isotope analyses reveal individual variability in the trophic ecology of a top marine predator, the southern elephant seal. Oecologia 169: 395–406

Hückstädt LA, Burns JM, Koch PL, McDonald BI, Crocker DE, Costa DP (2012b) Diet of a specialist in a changing environment: the crabeater seal along the western Antarctic Peninsula. Mar Ecol Prog Ser 455:287–301

Hussey NE, Kessel ST, Aarestrup K, Cooke SJ and others (2015) Aquatic animal telemetry: A panoramic window into the underwater world. Science 348:1255642

Jaeger A, Jaquemet S, Phillips RA, Wanless RM, Richard P, Cherel Y (2013) Stable isotopes document inter- and intra-specific variation in feeding ecology of nine large southern Procellariiformes. Mar Ecol Prog Ser 490: 255–266

Kernaléguen L, Cazelles B, Arnould JPY, Richard P and others (2012) Long-term species, sexual and individual variations in foraging strategies of fur seals revealed by stable isotopes in whiskers. PLOS ONE 7:e32916

Kirkman SP, Bester MN, Pistorius PA, Hofmeyr GJG, Jonker FC, Owen R, Strydom N (2003) Variation in the timing of moult in southern elephant seals at Marion Island. S Afr J Wildl Res 33:79–84

Lewis R, O'Connell TC, Lewis M, Campagna C, Hoelzel AR (2006) Sex-specific foraging strategies and resource partitioning in the southern elephant seal (*Mirounga leonina*). Proc R Soc B 273:2901–2907

Ling JK (1966) The skin and hair of the southern elephant seal, *Mirounga leonina* (Linn.) I. The facial vibrissae. Aust J Zool 14:855–866

Lowther AD, Harcourt RG, Goldsworthy SD (2013) Regional variation in trophic ecology of adult female Australian sea lions inferred from stable isotopes in whiskers. Wildl Res 40:303–311

McHuron EA, Walcott SM, Zeligs J, Skrovan S, Costa DP, Reichmuth C (2016) Whisker growth dynamics in two North Pacific pinnipeds: implications for determining foraging ecology from stable isotope analysis. Mar Ecol Prog Ser 554:213–224

McMahon KW, Hamady LL, Thorrold SR (2013) A review of ecogeochemistry approaches to estimating movements of marine animals. Limnol Oceanogr 58:697–714

Newland C, Field IC, Cherel Y, Guinet C, Bradshaw CJA, McMahon CR, Hindell MA (2011) Diet of juvenile southern elephant seals reappraised by stable isotopes in whiskers. Mar Ecol Prog Ser 424:247–258

Pistorius PA, de Bruyn PJN, Bester MN (2011) Population dynamics of southern elephant seals: a synthesis of three decades of demographic research at Marion Island. Afr J Mar Sci 33:523–534

Postma M, Bester MN, de Bruyn PJN (2013) Age-related reproductive variation in a wild marine mammal population. Polar Biol 36:719–729

R Core Team (2013) R: A language and environment for statistical computing. R Foundation for Statistical Computing, Vienna

Rea LD, Christ AM, Hayden AB, Stegall VK and others (2015) Age-specific vibrissae growth rates: A tool for determining the timing of ecologically important events in Steller sea lions. Mar Mamm Sci 31:1213–1233

Robertson A, McDonald RA, Delahay RJ, Kelly SD, Bearhop S (2013) Whisker growth in wild Eurasian badgers *Meles meles*: implications for stable isotope and bait marking studies. Eur J Wildl Res 59:341–350

Rohwer S, Ricklefs RE, Rohwer VG, Copple MM (2009) Allometry of the duration of flight feather molt in birds. PLOS Biol 7:e1000132

Sadou MC, Beltran RS, Reichmuth C (2014) A calibration procedure for measuring pinniped vibrissae using photogrammetry. Aquat Mamm 40:213–218

Tieszen LL, Boutton TW, Tesdahl KG, Slade NA (1983) Fractionation and turnover of stable carbon isotopes in animal tissues: implications for $\delta^{13}C$ analysis of diet. Oecologia 57:32–37

von Bertalanffy L (1938) A quantitative theory of organic growth. Hum Biol 10:181–213

Walters A (2014) Quantifying the trophic linkages of Antarctic marine predators. PhD thesis, University of Tasmania, Hobart

Walters A, Lea MA, van den Hoff J, Field IC, Virtue P, Sokolov S, Pinkerton MH, Hindell MA (2014) Spatially explicit estimates of prey consumption reveal a new krill predator in the Southern Ocean. PLOS ONE 9:e86452

Wilkinson IS, Bester MN (1990) Duration of post-weaning fast and local dispersion in the southern elephant seal, *Mirounga leonina*, at Marion Island. J Zool (Lond) 222: 591–600

Young JW, Hunt BPV, Cook TR, Llopiz JK and others (2015) The trophodynamics of marine top predators: current knowledge, recent advances and challenges. Deep-Sea Res II 113:170–187

Zhao L, Schell DM (2004) Stable isotope ratios in harbor seal *Phoca vitulina* vibrissae: effects of growth patterns on ecological records. Mar Ecol Prog Ser 281:267–273

Editorial responsibility: Yves Cherel, Villiers-en-Bois, France

Submitted: March 16, 2016; Accepted: September 21, 2016
Proofs received from author(s): October 28, 2016